PERGAMON

International Journal of Heat and Mass Transfer 44 (2001) 1889–1898

International Journal of HEAT and MASS TRANSFER

www.elsevier.com/locate/ijhmt

# Effect of ambient temperature on vertical turbulent buoyant water jets

Asterios Pantokratoras

*School of Engineering, Democritus University of Thrace, 67100 Xanthi, Greece*

Received 4 March 2000; received in revised form 10 July 2000

**Abstract**

Round and plane turbulent heated water jets discharged vertically into a stagnant uniform ambient water are considered. A differential turbulence model is used with numerical solution of the boundary layer equations. The International Equation of State for Seawater is used for the calculation of the buoyancy force. It is found that the buoyant jet characteristics are dependent on ambient water temperature due to nonlinear relationship between water density and temperature. This finding is of great practical importance for the design of thermal and wastewater diffusers. The design can be achieved efficiently using only mathematical models that include the water equation of state. © 2001 Elsevier Science Ltd. All rights reserved.

## 1. Introduction

Buoyancy plays an important role in a number of fluid flows of environmental importance. Examples include vertical motion of air in the atmosphere, spreading of smoke and other pollutants in the atmosphere and dispersal of volcano exhaust and water outfalls. Once the fluid is set into motion, its velocity field affects the thermal field and vice versa. The initial state of laminar motion very quickly changes into turbulence and the flow starts to spread radially by entrainment ambient fluid into the main flow.

The round turbulent plume has been a subject of investigation for more than 50 years. Rouse et al. [1] obtained similarity relations for round plumes and experimentally verified their functional forms. They generated plumes with gas burners and used thermocouples and wind-vane anemometers to measure the mean buoyancy and mean vertical velocity. George et al. [2] measured the mean and turbulence quantities in an air plume using hot-wire anemometry. Ogino et al. [3] used hot films and thermocouples to measure the centerline decay rates of velocity and temperature in thermal water buoyant jets. Kotsovinos [4] used thermistor probes to measure the temperature fields in thermal water buoyant jets and the same technique used by Papanicolaou and List [5] for the same problem. Papanicolaou and List [6] carried out a more comprehensive set of measurements using LDA and laser-induced fluorescence technique in salt water buoyant jets. Shabbir and George [7] used hot-wires to study the structure of hot vertical air plume. Dai et al. [8–11] studied the mixture fractions and velocities in round turbulent air plumes using laser velocimetry and laser-induced fluorescence.

Although existence of similarity has been confirmed in these experiments there has been some disagreement about the centerline values of the mean velocity and buoyancy profiles as well as the plume spreading rate. Shabbir and George [7] found substantial differences between their results and that of Papanicolaou and List [6]. The measured profiles are lower and wider than that of Papanicolaou and List [6]. On the other side Dai et al. found that self-preserving round turbulent plumes were narrower and had larger mean mixture fractions and streamwise velocities near the axis than that of Shabbir and George [7] in agreement with Papanicolaou and List [6]. They argue that most previous experiments have been conducted in the transitional region between jet and fully developed plume. Many comparisons made in the above works include both air and water plumes. The

*E-mail address:* pantokrator@xanthi.cc.duth.gr (A. Pantokratoras).


PII: S0017-9310(00)00231-3

**Nomenclature**

| | |
|---|---|
| $A_T$ | centerline buoyancy |
| $A_u$ | centerline dimensionless velocity |
| $b_{0.5T}$ | temperature half width |
| $b_{0.5u}$ | velocity half width |
| $B$ | specific buoyancy flux |
| $c_p$ | specific heat |
| $D$ | jet diameter or jet slot width |
| $F_o$ | initial densimetric Froude number |
| $g$ | gravitational acceleration |
| $k$ | turbulent kinetic energy |
| $K$ | mean bulk modulus |
| $l_M$ | characteristic length scale, $M^{3/4}/B^{1/2}$ |
| $l_Q$ | characteristic length scale, $Q/M^{1/2}$ |
| $M$ | jet specific momentum flux |
| $n$ | radial similarity variable |
| $p$ | pressure |
| $Q$ | jet volume flux at the orifice |
| $s$ | salinity |
| $T$ | water temperature |
| $T_a$ | ambient water temperature |
| $T_c$ | centerline water temperature |
| $T_o$ | initial water temperature |
| $\overline{T'^2}$ | mean square temperature fluctuation |
| $\overline{u^2}$ | vertical velocity fluctuation |
| $\overline{uv}$ | turbulent shear stress |
| $\overline{uT'}$ | vertical turbulent heat flux |
| $U$ | vertical mean velocity |
| $U_c$ | centerline vertical mean velocity |
| $U_o$ | jet exit velocity |
| $\overline{v^2}$ | horizontal velocity fluctuation |
| $\overline{vT'}$ | horizontal turbulent heat flux |
| $V$ | horizontal mean velocity |
| $W$ | specific volume |
| $x$ | vertical coordinate |
| $y$ | horizontal coordinate |

*Greek symbols*

| | |
|---|---|
| $\alpha$ | thermal expansion coefficient of water |
| $\beta$ | local buoyancy flux |
| $\varepsilon$ | kinetic energy dissipation |
| $\lambda$ | ratio of temperature width to velocity width |
| $\xi$ | dimensionless distance from the nozzle |
| $\rho$ | water density |
| $\rho_a$ | ambient water density |
| $\rho_c$ | water density at plume axis |
| $\rho_o$ | initial water density |

*Subscripts*

| | |
|---|---|
| c | centerline value |
| o | initial value |
| a | ambient value |

*Superscripts*

| | |
|---|---|
| $i = 0$ | for plane plumes |
| $i = 1$ | for round plumes |

purpose of this paper is to show that the water plume behavior is dependent on ambient temperature in contrary to air plumes. Consequently, the comparison between water and air plumes must be done carefully.

## 2. Analysis

Round buoyant jets can be parameterized in terms of their fluxes of mass, momentum and density deficiency (or buoyancy flux). If $Q$ is the volume rate of flow, $M$ the specific momentum flux and $B$ is the specific buoyancy flux then the following definitions relate $Q$, $M$ and $B$

$$Q = \pi \frac{D^2}{4} U_o, \tag{1}$$

$$M = Q U_o, \tag{2}$$

$$B = Q \frac{\rho_a - \rho_o}{\rho_a} g, \tag{3}$$

where $D$ is the jet diameter, $U_o$ the jet exit velocity and $\rho_o$ and $\rho_a$ are jet exit and ambient density, respectively. From the above quantities two characteristic length scales are defined [5]

$$l_Q = \frac{Q}{M^{1/2}} \quad \text{and} \quad l_M = \frac{M^{3/4}}{B^{1/2}}. \tag{4}$$

The dimensionless elevation from the jet is defined as

$$\xi = \frac{x}{l_M} = \left(\frac{\pi}{4}\right)^{-1/4} \frac{1}{F_o} \frac{x}{D}, \tag{5}$$

where $x$ is the elevation from the jet nozzle and $F_o$ is the initial densimetric Froude number given by the following equation:

$$F_o = U_o \Big/ \left( \frac{\rho_a - \rho_o}{\rho_a} g D \right)^{1/2}. \tag{6}$$

The basic controlling parameter determining whether a round buoyant jet behaves like jet or plume is the quantity $\xi$. According to Papanicolaou and List [5] for values of $\xi > 5$ the buoyant jet behaves like a plume and for $\xi < 1$ like a jet. For $1 < \xi < 5$ the buoyant jet is in a transitional region. On the other side Dai and Faeth [11] suggest that self-preservation is reached only when $x/D > 87$ and $\xi > 12$ according to their measurements in round air plumes.

It is known in the literature that there are similarity solutions for the round and plane turbulent plumes. The similarity relationships for the mean buoyancy and ve-

locity proposed by Shabbir and George [7] for round plumes are

$$g(\rho_a - \rho)/\rho_a B^{-2/3} x^{5/3} = A_T \exp(-68n^2), \tag{7}$$

$$UB^{-1/3} x^{1/3} = A_u \exp(-58n^2), \tag{8}$$

where $U$ is the plume streamwise mean velocity and $n$ is the radial similarity variable equal to $r/x$. The constants $A_T$ and $A_u$ are determined experimentally. The buoyancy flux for air plumes is constant and equal to its initial value. For $n = 0$ Eqs. (7) and (8) take the following form:

$$A_T = g(\rho_a - \rho_c)/\rho_a B^{-2/3} x^{5/3}, \tag{9}$$

$$A_u = U_c B^{-1/3} x^{1/3}, \tag{10}$$

where $\rho_c$ and $U_c$ is the centerline plume density and velocity. $A_T$ and $A_u$ calculated by Shabbir and George for air plumes are 9.4 and 3.4, respectively. Eq. (9) can be written as follows for water plumes

$$A_T = g\alpha(T_c)(T_c - T_a)\beta^{-2/3} x^{5/3}, \tag{11}$$

where $\alpha(T_c)$ is the water thermal expansion coefficient calculated at the local centerline temperature, $T_c$ and $T_a$ are the plume centerline and ambient temperature and $\beta$ is the local buoyancy flux. The initial buoyancy flux $B$ has been replaced by the local buoyancy flux because this quantity is not constant in water plumes. The local buoyancy flux is related to the conserved heat flux $H$ by the following relation [4]

$$\beta = \alpha(T_c)\frac{gH}{\rho c_p} = \alpha(T_c) g\pi \frac{D^2}{4} U_o (T_o - T_a). \tag{12}$$

From Eq. (12) it is clear that buoyancy flux is not conserved in a thermal water plume because $\alpha(T_c)$ is a function of temperature and decreases as the temperature decreases. Substituting $\beta$ from (12) into (11) yields

$$A_T = \alpha(T_c)^{1/3}(T_c - T_a) x^{5/3} g^{1/3} \left(\pi \frac{D^2}{4} U_o (T_o - T_a)\right)^{-2/3}. \tag{13}$$

From the above equation it is clear that $A_T$ is proportional to $\alpha(T_c)^{1/3}$. It is well known that in a thermal turbulent buoyant jet the temperature drops rapidly in the initial region due to entrainment and afterwards the jet temperature approaches the ambient temperature asymptotically. In the plume region, where similarity exists, the centerline temperature is very close to ambient temperature. This means also that in a turbulent water plume $\alpha(T_c)$ is very close to $\alpha(T_a)$. However, it is known that water thermal expansion coefficient decreases as the temperature decreases and becomes zero at 4°C. Consequently, $A_T$ is not a constant for water plumes as it was believed until now. Taking into account that $\alpha(T_c) \cong \alpha(T_a)$ it is seen that $A_T$ is essentially a function of the plume ambient temperature and decreases as the plume ambient temperature approaches 4°C.

Following the above procedure we obtain the following relation for $A_u$

$$A_u = \alpha(T_c)^{-1/3} U_c x^{1/3} g^{-1/3} \left(\pi \frac{D^2}{4} U_o (T_o - T_a)\right)^{-1/3}. \tag{14}$$

From this equation it is seen that $A_u$ also is not a constant for water plumes. Taking into account that $\alpha(T_c) \cong \alpha(T_a)$ it is seen that $A_u$ is also a function of the plume ambient temperature and increases as the plume ambient temperature approaches 4°C.

The above analysis is valid also for velocity and temperature fluctuations. These quantities in similarity form are given by Shabbir and George [7]. The temperature variance $g^2\alpha(T)^2\overline{T'^2}\beta^{-4/3}x^{10/3}$, the vertical turbulent heat flux $\overline{uT'}\beta^{-1}x^2$, the radial turbulent heat flux $\overline{vT'}\beta^{-1}x^2$, the vertical velocity fluctuation $\overline{u^2}\beta^{2/3}x^{2/3}$, the radial velocity fluctuation $\overline{v^2}\beta^{-2/3}x^{2/3}$ and the turbulent shear stress $\overline{uv}\beta^{-2/3}x^{2/3}$ are all functions of the buoyancy flux $\beta$ which is a function of the water thermal expansion coefficient $\alpha(T)$. Taking into account that $\alpha(T) \cong \alpha(T_a)$ it is seen that all the above quantities are functions of the plume ambient temperature. For example the temperature variance takes the following form

$$g^2\alpha(T)^2\overline{T'^2}\beta^{-4/3}x^{10/3} = g^{2/3}\alpha(T)^{2/3}\overline{T'^2} \times \left(\pi \frac{D^2}{4} U_o (T_0 - T_a)\right)^{-4/3} x^{10/3}. \tag{15}$$

This quantity is proportional to $\alpha(T)^{2/3}$ and consequently decreases as the plume ambient temperature approaches 4°C.

For plane turbulent plumes the corresponding $\xi$ parameter determining whether a buoyant jet behaves like jet or plume is [12]

$$\xi = \frac{1}{F_o^{4/3}} \frac{x}{D}, \tag{16}$$

where $D$ is the slot width. The constants $A_T$ and $A_u$ are

$$A_T = g\alpha(T_c)(T_c - T_a)\beta^{-2/3} x, \tag{17}$$

$$A_u = U_c \beta^{-1/3}. \tag{18}$$

Following the above procedure we obtain the following relations for $A_T$ and $A_u$

$$A_T = \alpha(T_c)^{1/3}(T_c - T_a) x g^{1/3} (D U_o (T_o - T_a))^{-2/3}, \tag{19}$$

$$A_u = \alpha(T_c)^{-1/3} U_c g^{-1/3} (D U_o (T_o - T_a))^{-1/3}. \tag{20}$$

From these relations it is also clear that $A_T$ and $A_u$ are functions of the plume ambient temperature.

The dependence of $A_T$ and $A_u$ on ambient temperature is weak at high temperatures where the water density–temperature relationship is linear and becomes stronger as the ambient temperature approaches the maximum density temperature (4°C) where the density–temperature relationship is nonlinear. This is maybe the reason that this dependence has not been identified until now. For the three experimental works concerning round water thermal plumes most frequently cited in the literature, the ambient temperatures were the following. Ogino et al. [3] mention that the ambient water temperature of their experiments ranged between 12°C and 27°C but they did not give more details. In Kotsovinos [4] measurements the water ambient temperature was kept between 20°C and 23°C. Papanicolaou and List [5] used ambient water temperatures between 23.90°C and 15.25°C. The most important experimental works concerning plane water thermal plumes are those of Kotsovinos [12] and Ramaprian and Chandrasekhara [13]. In Kotsovinos measurements the water ambient temperature was kept between 21°C and 25°C while Ramaprian and Chandrasekhara used ambient temperatures between 21.1°C and 24.4°C.

At these ambient temperatures it is difficult to identify the influence of $T_a$ on $A_T$ and $A_u$ taking into account the unavoidable experimental scatter.

## 3. The mathematical model

Experimental data for thermal water plumes at low ambient temperatures have not been reported in the literature. For that reason a mathematical model will be used in this work in order to study the problem of plume behavior at low ambient temperatures.

Consider a vertical turbulent jet discharging into a calm environment with $U$ and $V$ denoting respectively the mean velocity components in the $x$ and $y$ direction, where $x$ is vertically upwards and $y$ is the coordinate perpendicular to $x$. The flow is assumed to be steady, of the boundary-layer type. The governing equations of this flow with Boussinesq approximations are:

$$\text{continuity equation :} \qquad \frac{\partial U}{\partial x}+\frac{1}{y^i}\frac{\partial (y^i V)}{\partial y}=0, \tag{21}$$

momentum equation :

$$U\frac{\partial U}{\partial x}+V\frac{\partial U}{\partial y}=\frac{1}{y^i}\frac{\partial}{\partial y}(-y^i\overline{uv})-\frac{\rho-\rho_a}{\rho_a}g, \tag{22}$$

energy equation :

$$U\frac{\partial T}{\partial x}+V\frac{\partial T}{\partial y}=\frac{1}{y^i}\frac{\partial}{\partial y}\left(-y^i\overline{vT'}\right). \tag{23}$$

The superscript $i$ is zero for plane jets and 1 for round jets. The density of water, which is included in (22), is generally a function of temperature, salinity and pressure. In this paper the known from Oceanography International Equation of State for Seawater [14] is used for the calculation of density from temperature, salinity and pressure. The following equation is used

$$\rho(s,T,p)=1/W(s,T,p), \tag{24}$$

where $W(s,T,p)$ is the specific volume. The specific volume is calculated by

$$W(s,T,p)=W(s,T,0)[1-p/K(s,T,p)], \tag{25}$$

where $K(s,T,p)$ is the mean bulk modulus. The bulk modulus is calculated by

$$K(s,T,p)=E+Fs+Gs^{3/2}+\left(H+Is+Js^{3/2}\right)p+(M+Ns)p^2. \tag{26}$$

The specific volume at atmospheric pressure is calculated by

$$W(s,T,0)=1/\left(A+Bs+Cs^{3/2}+Ds^2\right). \tag{27}$$

In the above equations the coefficients $A,B,C,D,E,F,G,H,I,J,M$ and $N$ are polynomials in temperature. The calculation procedure is the following: First the specific volume at atmospheric pressure and the mean bulk modulus are calculated, then it is calculated the specific volume and finally the density. The equation of state for seawater is valid for temperatures from −2°C to 40°C, salinities from 0‰ to 40‰ and pressures from 1 to maximum oceanic pressure in bars. In this paper all calculations have been made for zero salinity and atmospheric pressure, that is for 1 bar.

The two turbulent quantities $\overline{uv},\overline{vT'}$ shown in (22) and (23) are the turbulent shear stress and heat flux, respectively. In order to solve Eqs. (21)–(23), a turbulence closure model for these fluxes has to be specified. In the current work, the model proposed by Chen and Chen [15] is adopted. The model is referred briefly as the $k$–$\varepsilon$–$\overline{T'^2}$. The differential equations for the $k$–$\varepsilon$–$\overline{T'^2}$ model, under the boundary-layer approximation, are as follows:

$$U\frac{\partial k}{\partial x}+V\frac{\partial k}{\partial y}=\frac{1}{y^i}\frac{\partial}{\partial y}\left(y^i c_k\frac{k\overline{v^2}}{\varepsilon}\frac{\partial k}{\partial y}\right)-\overline{uv}\frac{\partial U}{\partial y}+\alpha(T)g\overline{uT'}-\varepsilon, \tag{28}$$

$$U\frac{\partial \varepsilon}{\partial x}+V\frac{\partial \varepsilon}{\partial y}=\frac{1}{y^i}\frac{\partial}{\partial y}\left(y^i c_\varepsilon\frac{k\overline{v^2}}{\varepsilon}\frac{\partial \varepsilon}{\partial y}\right)+c_{\varepsilon 1}\frac{\varepsilon}{k}\times\left(-\overline{uv}\frac{\partial U}{\partial y}+\alpha(T)g\overline{uT'}\right)-c_{\varepsilon 2}\frac{\varepsilon^2}{k}, \tag{29}$$

$$U\frac{\partial\overline{T'^2}}{\partial x}+V\frac{\partial\overline{T'^2}}{\partial y}=\frac{1}{y^i}\frac{\partial}{\partial y}\left(y^i c_T\frac{k^2}{\varepsilon}\frac{\partial\overline{T'^2}}{\partial y}\right)-2\overline{vT'}\frac{\partial T}{\partial y}-c_{T1}\frac{\varepsilon\overline{T'^2}}{k}, \tag{30}$$

where $k$ is the turbulent kinetic energy ($k=(1/2)\overline{u_iu_i}$) and $\varepsilon$ is the dissipation of that energy

$$\left(\varepsilon=v\overline{\frac{\partial u_i}{\partial x_k}\frac{\partial u_i}{\partial x_k}}\right).$$

$\overline{T'^2}$ is the fluctuating temperature and $\alpha(T)$ is the thermal expansion coefficient of water defined as

$$\alpha(T)=-\frac{1}{\rho}\frac{\partial\rho}{\partial T}. \tag{31}$$

In this work the thermal expansion coefficient of water at any temperature $T_1$ was calculated from the following equation

$$\alpha(T_1)=-\frac{1}{\rho_1}\frac{\rho_2-\rho_1}{T_2-T_1}, \tag{32}$$

where $\rho_1$ and $\rho_2$ are the densities corresponding to temperature $T_1$ and $T_2$ ($T_2=T_1+0.01$°C). The densities were calculated using the International Equation of State for Seawater.

The following approximated algebraic relations for the $\overline{uv}, \overline{v^2}, \overline{vT'}, \overline{uT'}$ are used

$$-\overline{uv}=\frac{1-c_o}{c_1}\frac{\overline{v^2}}{k}\left(1+\frac{\alpha(T)kg(\partial T/\partial y)}{c_h\varepsilon(\partial U/\partial y)}\right)\frac{k^2}{\varepsilon}\frac{\partial U}{\partial y}, \tag{33}$$

$$\overline{v^2}=c_2k, \tag{34}$$

$$-\overline{vT'}=\frac{1}{c_h}\frac{\overline{v^2}}{k}\frac{k^2}{\varepsilon}\frac{\partial T}{\partial y}, \tag{35}$$

$$\overline{uT'}=\frac{k}{c_h\varepsilon}\left(-\overline{uv}\frac{\partial T}{\partial y}-\overline{vT'}(1-c_{h1})\frac{\partial U}{\partial y}+\alpha(T)g(1-c_{h1})\overline{T'^2}\right). \tag{36}$$

In the above $k$–$\varepsilon$–$\overline{T'^2}$ turbulent model eleven (11) empirical constants are included. Chen and Chen [15] used the following constants.

| $c_o$ | $c_1$ | $c_2$ | $c_\varepsilon$ | $c_{\varepsilon1}$ | $c_{\varepsilon2}$ |
|---|---|---|---|---|---|
| 0.55 | 2.2 | 0.53 | 0.15 | 1.43 | 1.92 |
| $c_k$ | $c_T$ | $c_{T1}$ | $c_h$ | $c_{h1}$ | |
| 0.225 | 0.13 | 1.25 | 3.2 | 0.5 | |

Although more powerful and sophisticated turbulent models have been developed in recent years and some of the above constants have been modified [16–20], in the present work the same constants used by Chen and Chen [15] have been used because the main purpose of this work is to study the influence of the water equation of state and thermal expansion coefficient on plume characteristics.

Boundary conditions are applied at the edge and at the axis of the buoyant jet as follows:

$$x>0,\quad y=0,\quad \frac{\partial}{\partial y}\left(T,U,k,\varepsilon,\overline{T'^2}\right)=0, \tag{37}$$

$$x>0,\quad y\to\infty,\quad T=T_a,\quad U=k=\varepsilon=\overline{T'^2}=0. \tag{38}$$

At the beginning of the computation, the exit mean velocity and temperature profiles, the turbulent kinetic energy, its dissipation rate and the temperature fluctuation must be specified. For velocity and temperature distribution flat profiles are assumed. The literature on experimental measurements did not provide the profiles for the initial turbulent kinetic energy, its dissipation function and the temperature fluctuation profile. In the present analysis, Gaussian profiles were assumed for $k_o, \varepsilon_o, \overline{T_o'^2}$.

Eqs. (21)–(23) and (28)–(30) form a parabolic system and are solved by a method described by Patankar [21]. The finite difference method is used with primitive variables $x$, $y$ and a space marching procedure is used in $x$ direction. Calculations have been performed over half of the jet as the flow is symmetric. The inlet plane has been located at the exit, where the outer boundary of the calculation domain is located at $y/D=1$. An expanding grid has been used according to the following relation

$$y_{out}=y_{in}+cx, \tag{39}$$

where $y_{in}$ is the location of the outer boundary at jet exit, $c$ the spreading rate of the outer boundary and $x$ is the distance at the current step. The appropriate value of $c$ has been found to be 0.20. The forward step size increases in proportion to the width of the calculation domain and the lateral cells are distributed uniformly. In this work the forward step was 1% of the outer boundary and a total of 300 lateral grid cells have been used. For more information about the expanding grid, see [22]. Calculations were made on a DEC ALPHA 7000 computer using quadruple precision accuracy.

## 4. Results and discussion

### 4.1. Round buoyant jets

In Figs. 1 and 2 the variation of $A_T$ with $\xi$ for different ambient water temperatures and initial Froude numbers 5 and 10, respectively are shown. These curves have been produced using the above described mathematical model. From these figures some very interesting conclusions can be drawn.

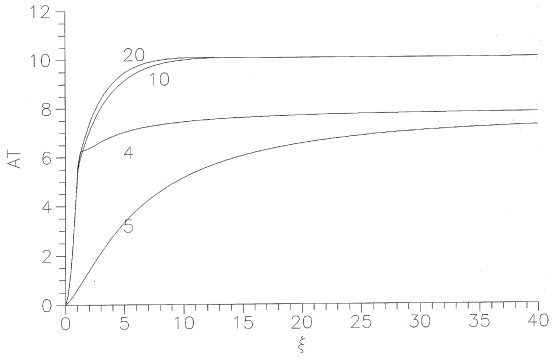


Fig. 1. Variation of centerline buoyancy in round buoyant jets for $F_o = 5$. Numbers near curves indicate ambient temperatures.

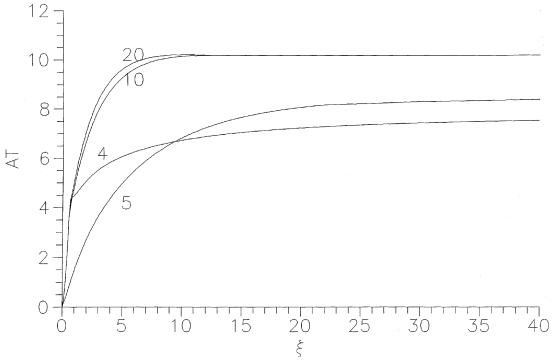


Fig. 2. Variation of centerline buoyancy in round buoyant jets for $F_o = 10$. Numbers near curves indicate ambient temperatures.

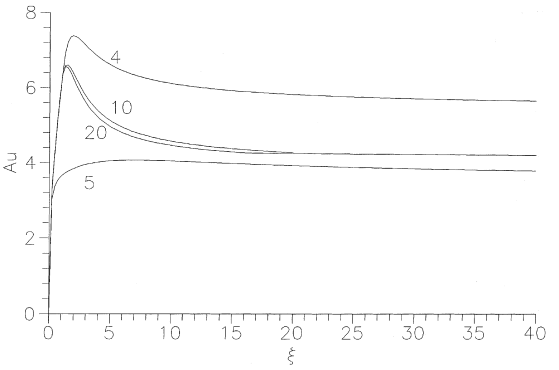


Fig. 3. Variation of centerline dimensionless velocity in round buoyant jets for $F_o = 5$. Numbers near curves indicate ambient temperatures.

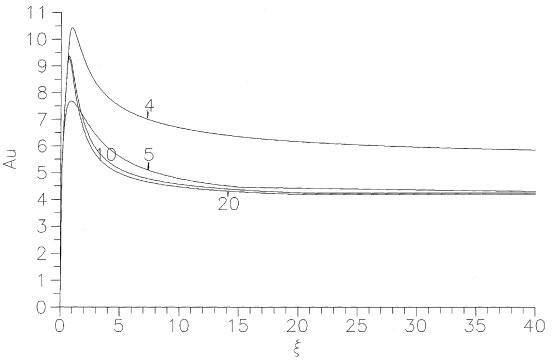


Fig. 4. Variation of centerline dimensionless velocity in round buoyant jets for $F_o = 10$. Numbers near curves indicate ambient temperatures.

1. It is clear that as $\xi$ increases the $A_T$ parameter approaches a constant value and the plume approaches the self-preserving state.

2. At high ambient water temperatures where the density–temperature relationship is linear all $A_T$ values collapse to the same value independent of initial Froude number and ambient water temperature. In contrary, at ambient temperatures around the density extremum temperature, $A_T$ values depend on ambient water temperature and initial Froude number. Generally the $A_T$ plume value decreases as the ambient temperature decreases according to the previous analysis but this trend is not monotonic. For example, for $F_o = 5$ the $A_T$ value that corresponds to $T_a = 4°C$ is bigger than that of $T_a = 5°C$.

3. At high ambient water temperatures the required $\xi$ value for reaching self-preservation is almost constant and equal to about 12. At ambient temperatures around the density extremum temperature, the required $\xi$ value is again a function of ambient water temperature and initial Froude number. In this region these values are much greater. For example, for $F_o = 5$ and $T_a = 5°C$ this value is about 30. Thus the Dai and Faeth [11] suggestion that self-preservation is reached when $x/D > 87$ and $\xi > 12$ is not valid for round water plumes at low ambient temperatures. In Figs. 3 and 4 the variation of $A_u$ with $\xi$ for different ambient water temperatures and initial Froude numbers 5 and 10, respectively are shown. The above mentioned conclusions are also valid for $A_u$ values. At ambient temperatures around the density extremum temperature, $A_u$ depend on ambient water temperature and initial Froude number and generally increases as the ambient water temperature decreases. In Table 1 the values of $A_T$ and $A_u$ calculated by the present work for $F_o = 10$ are shown in comparison with the existing values in the literature.

In Figs. 5 and 6 the lateral mean buoyancy $g(\rho_a - \rho)/\rho_a \beta^{-2/3} x^{5/3}$ and mean velocity $U\beta^{-1/3}x^{1/3}$ profiles are shown for $F_o = 10$ and $T_a = 20°C$, 10°C, 5°C

Table 1
Summary of mean flow centerline buoyancy and velocity parameters for round plumes

| Reference | $A_T$ | $A_u$ |
|---|---|---|
| Rouse et al. [1] (air) | 11.00 | 4.70 |
| George et al. [2] (air) | 9.10 | 3.40 |
| Ogino et al. [3] (water) | 9.40 | – |
| Chen and Rodi [23] (review) | 9.35 | 3.50 |
| Kotsovinos [4] (water) | 8.80 | – |
| Papanicolaou and List [5] (water) | 11.11 | – |
| Papanicolaou and List [6] (water) | 14.28 | 3.85 |
| Shabbir and George [7] (air) | 9.40 | 3.40 |
| Dai and Faeth [11] (air) | 12.60 | 4.30 |
| Present study for $F_o = 10$ | | |
| Water at $T_a = 20°C$ | 10.20 | 4.20 |
| Water at $T_a = 10°C$ | 10.18 | 4.25 |
| Water at $T_a = 5°C$ | 8.20 | 4.50 |
| Water at $T_a = 4°C$ | 7.52 | 5.85 |

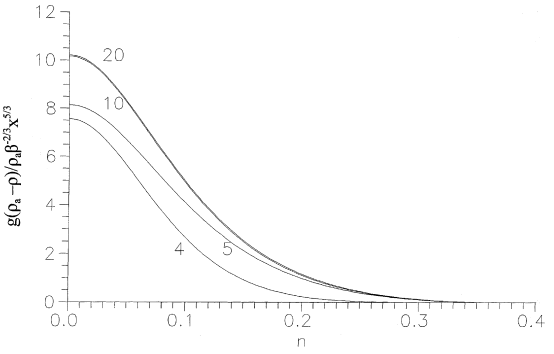


Fig. 5. Dimensionless buoyancy distribution across the round plumes for $F_o = 10$. Numbers near curves indicate ambient temperatures.

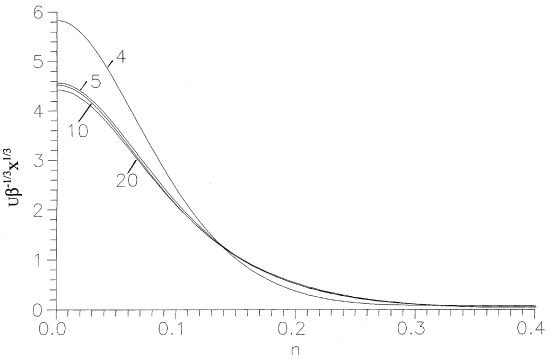


Fig. 6. Dimensionless velocity distribution across the round plumes for $F_o = 10$. Numbers near curves indicate ambient temperatures.

and 4°C. From these figures it is clear that the buoyancy decreases as the ambient temperature decreases and the profiles become narrower while the dimensionless

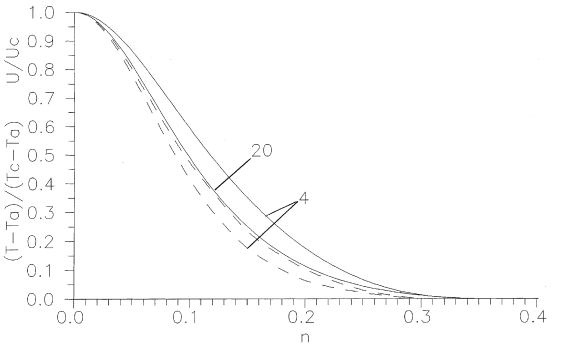


Fig. 7. Dimensionless temperature and velocity profiles in round plumes for $F_o = 10$ and $T_a = 20°C$ and 4°C. Solid line curves correspond to temperature and dashed lines to velocity.

velocity $U\beta^{-1/3}x^{1/3}$ increases and the profiles become wider.

In Fig. 7 the lateral dimensionless temperature $(T - T_a)/(T_c - T_a)$ and mean velocity $U/U_c$ profiles are shown for $F_o = 10$ and $T_a = 20°C$ and 4°C. From this figure it is seen that the temperature profiles become wider as the ambient temperature decreases while the velocity profiles become narrower. It is seen also that the temperature profile is always wider than the corresponding velocity profile but this relation is dependent on ambient temperature. At $T_a = 4°C$ the temperature profile is much wider than that of velocity compared to that of $T_a = 20°C$. The ratio of temperature half-width to velocity half-width ($\lambda = b_{0.5T}/b_{0.5U}$) is 1.05 at $T_a = 20°C$ and 1.37 at $T_a = 4°C$. Integral models used for design calculations like those evaluated by Alam et al. [24] use a constant $\lambda$ value independent of ambient conditions. Consequently, these models can be used at low ambient water temperatures only when a variable $\lambda$ is adopted.

The variation of temperature and velocity half-width as function of $x/D$ for $T_a = 20°C$ and 4°C is illustrated by Fig. 8 for $F_o = 10$. The temperature half-width becomes greater as the ambient temperature decreases while the velocity half-width decreases.

In Fig. 9 the centerline temperature dilution $(T_o - T_a)/(T_c - T_a)$ and the corresponding centerline density dilution $(\rho_a - \rho_o)/(\rho_a - \rho_c)$ are shown for $F_o = 10$ and different ambient temperatures. From this figure it is seen that both dilutions are also a function of ambient water temperature. The temperature dilution decreases while the density dilution increases as the ambient temperature decreases.

The mathematical model has also been used for the calculation of velocity and temperature fluctuations in similarity form given by Shabbir and George [7]. However, it is known that the measurement and simulation of turbulent quantities are more difficult than those of mean values and the discrepancies among various

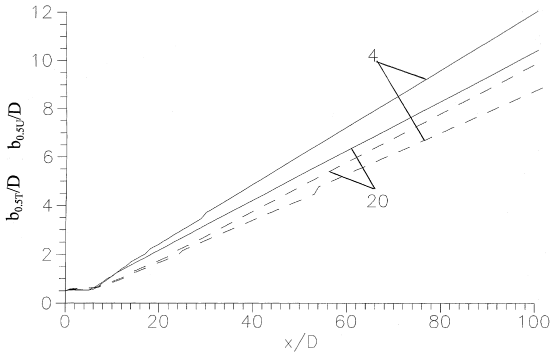


Fig. 8. Temperature and velocity half-width in round buoyant jets for $F_o = 10$ and $T_a = 20°C$ and 4°C. Solid line curves correspond to temperature and dashed lines to velocity.

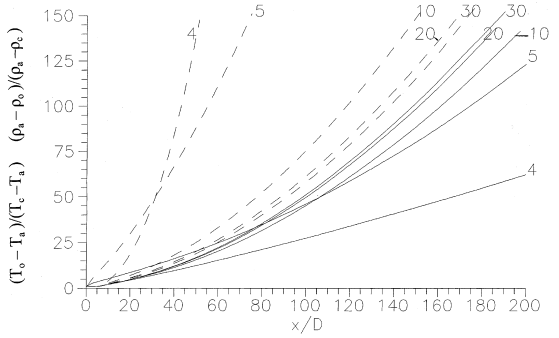


Fig. 9. Centerline dilution in round buoyant jets for $F_o = 10$. Solid lines correspond to temperature dilution and dashed lines to density dilution. Numbers near curves indicate ambient temperatures.

investigations are greater. There are either small or great discrepancies between the predicted and measured quantities by Shabbir and George [7] but the most important is the confirmation of the dependence of these quantities on ambient water temperature. For example, the centerline value of temperature variance $g^2\alpha(T)^2\overline{T'^2}\beta^{-4/3}x^{10/3}$ calculated at $T_a = 4°C$ is 83% lower than that which corresponds to $T_a = 20°C$ for the same Froude number ($F_o = 10$). This reduction is in accordance with the above finding that this quantity decreases as the ambient temperature decreases.

### 4.2. Plane buoyant jets

In Figs. 10 and 11 the variation of $A_T$ and $A_u$ with $\xi$ for different ambient water temperatures and initial Froude numbers 5 and 10, respectively are shown. These figures show again the dependence of $A_T$ and $A_u$ on ambient water temperature but there is no significant dependence on initial Froude number as is the case in

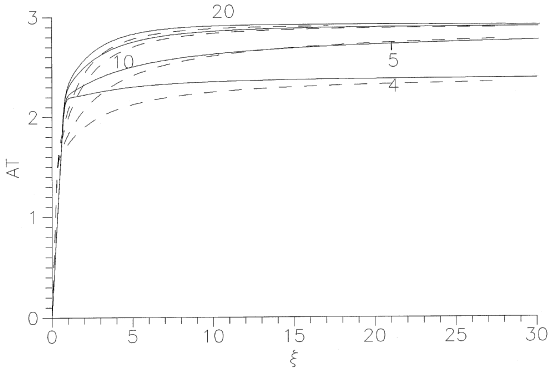


Fig. 10. Variation of centerline buoyancy in plane buoyant jets for $F_o = 5$ and 10. Solid line curves correspond to $F_o = 5$ and dashed lines to $F_o = 10$. Numbers near curves indicate ambient temperatures.

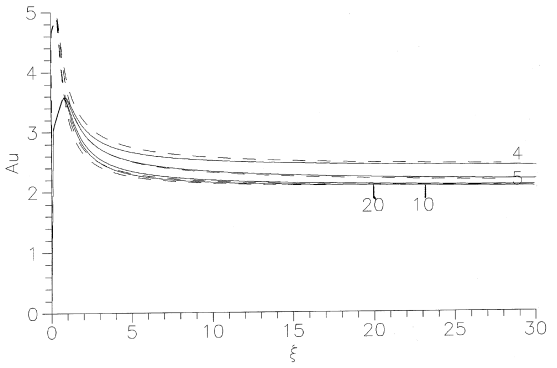


Fig. 11. Variation of centerline dimensionless velocity in plane buoyant jets for $F_o = 5$ and 10. Solid line curves correspond to $F_o = 5$ and dashed lines to $F_o = 10$. Numbers near curves indicate ambient temperatures.

Table 2
Summary of mean flow centerline buoyancy and velocity parameters for plane plumes

| Reference | $A_T$ | $A_u$ |
|---|---|---|
| Rouse et al. [1] (air) | 2.60 | 1.80 |
| Kotsovinos [12] (water) | 2.38 | 1.66 |
| Chen and Rodi [23] (review) | 2.40 | 1.90 |
| Ramaprian and Chandrasekhara [13] (water) | 2.56 | 2.13 |
| Present study for $F_o = 5$ and 10 | | |
| Water at $T_a = 20°C$ | 2.90 | 2.08 |
| Water at $T_a = 10°C$ | 2.89 | 2.09 |
| Water at $T_a = 5°C$ | 2.77 | 2.17 |
| Water at $T_a = 4°C$ | 2.32 | 2.44 |

round buoyant jets. In Table 2 the values of $A_T$ and $A_u$ calculated by the present method are shown in comparison with the existing values in the literature.

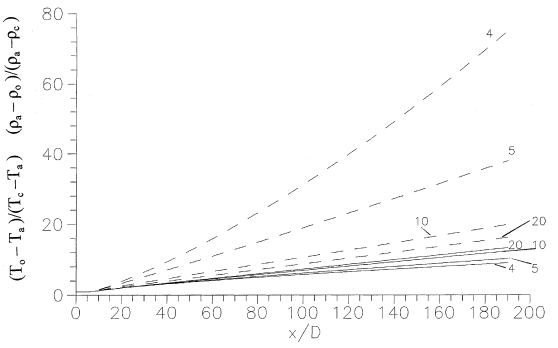


Fig. 12. Centerline dilution in plane buoyant jets for $F_o = 10$. Solid lines correspond to temperature dilution and dashed lines to density dilution. Numbers near curves indicate ambient temperatures.

Results were also produced for lateral dimensionless temperature $(T - T_a)/(T_c - T_a)$ and mean velocity $U/U_c$ profiles. The results are similar to that of round plumes. The temperature profiles become wider as the ambient temperature decreases while the velocity profiles become narrower. The temperature profiles are always wider than velocity profiles and $\lambda$ is dependent again on ambient temperature.

In Fig. 12 the centerline temperature dilution $(T_o - T_a)/(T_c - T_a)$ and the corresponding centerline density dilution $(\rho_a - \rho_o)/(\rho_a - \rho_c)$ are shown for $F_o = 10$ and different ambient temperatures. From this figure it is seen that both dilutions are also a function of ambient water temperature. Another interesting conclusion drawn from this figure is that the dependence of centerline temperature dilution on ambient temperature is not so strong as in the case of round plumes and that for the same initial Froude number, the same ambient temperature and the same axial distance, dilution in round plumes is much greater than that of plane plumes.

An interesting question arising from the above analysis is the following. When water plumes behave like air plumes and when they do not? For example, the lateral mean buoyancy $g(\rho_a - \rho)/\rho_a\beta^{-2/3}x^{5/3}$ profiles of round plumes are almost identical for ambient temperatures greater than 10°C (Fig. 5) and it could be claimed that in this region round water plumes behave like air plumes concerning this quantity. The mean velocity $U\beta^{-1/3}x^{1/3}$ profiles are almost identical for ambient temperatures greater than 5°C (Fig. 6). The situation is quite different concerning the centerline temperature dilution $(T_o - T_a)/(T_c - T_a)$ and the centerline density dilution $(\rho_a - \rho_o)/(\rho_a - \rho_c)$ (Fig. 9). It is known that for air plumes the two dilutions are almost identical independent of the ambient temperature, i.e.,

$$\frac{\rho_a - \rho_o}{\rho_a - \rho_c} \cong \frac{T_o - T_a}{T_c - T_a}. \tag{40}$$

From Fig. 9 it is seen that for round water plumes the two dilutions are close to each other only for $T_a > 30$°C and this is valid only for small distances from the jet nozzle. Things are better for plane plumes. The lateral mean buoyancy $g(\rho_a - \rho)/\rho_a\beta^{-2/3}x$ and velocity profiles $U\beta^{-1/3}$ of plane plumes are almost identical for ambient temperatures greater than 10°C and it could be claimed that in this region plane water plumes behave like air plumes. In addition, centerline temperature and density dilutions (Fig. 12) are close to each other for $T_a > 20$°C. In conclusion it could be claimed that round water plumes behave like air plumes for $T_a > 30$°C and plane plumes for $T_a > 20$°C.

The effect of ambient water temperature on centerline dilution in water buoyant jets is of great importance for practical applications. For example a water plume discharging from a thermal power plant diffuser has smaller centerline temperature dilution in winter than in summer for the same Froude number. This conclusion has also great importance for wastewater diffusers. In this case of great importance is the dilution of a passive tracer like BOD or a toxic substance which is carried by the plume flow. If there is a temperature difference between the discharge and the ambient water (and this happens in most cases) the centerline temperature dilution will be smaller in winter than in summer for the same initial Froude number. The corresponding centerline density dilution will be larger in winter than in summer and this is valid also for the passive tracer dilution which is assumed to be equal to $(\rho_a - \rho_o)/(\rho_a - \rho_c)$. It is advocated here that, all mathematical models available for the calculation of dilution from diffusers, which do not include the water equation of state, are unsuitable to predict the dilution efficiently when a temperature difference exists between the discharge and the ambient water.

## 5. Conclusions

The main finding of this work is the dependence of water buoyant jets behavior on ambient water temperature. The centerline similarity plume values of mean buoyancy and mean velocity, the lateral dimensionless temperature and mean velocity profiles, the temperature and velocity jet width, the spreading ratio between the temperature and velocity profile and the centerline temperature and density dilution are all functions of ambient water temperature. This dependence is due to nonlinear relationship between water density and temperature. This finding is of great practical importance for the design of thermal and wastewater diffusers which can be achieved using mathematical models that include the water equation of state.

## References


[1] H. Rouse, C.S. Yih, H.W. Humphreys, Gravitational convection from a boundary source, Tellus 4 (1952) 201–210.

[2] W.K. George, R.L. Alpert, F. Tamanini, Turbulence measurements in an axisymmetric buoyant plume, Int. J. Heat Mass Transfer 20 (1977) 1145–1154.

[3] F. Ogino, H. Takeuchi, I. Kudo, T. Mizushina, Heated jet discharged vertically into ambients of uniform and linear temperature profiles, Int. J. Heat Mass Transfer 23 (1980) 1581–1588.

[4] N.E. Kotsovinos, Temperature measurements in a turbulent round plume, Int. J. Heat Mass Transfer 28 (1985) 771–777.

[5] P.N. Papanicolaou, E.J. List, Statistical properties of tracer concentration in round buoyant jets, Int. J. Heat Mass Transfer 30 (1987) 2059–2071.

[6] P.N. Papanicolaou, E.J. List, Investigations of round turbulent buoyant jets, J. Fluid Mech. 195 (1988) 341–391.

[7] A. Shabbir, W.K. George, Experiments on a round turbulent buoyant plume, J. Fluid Mech. 275 (1994) 1–32.

[8] Z. Dai, L.K. Tseng, G.M. Faeth, Structure of round, fully feveloped, buoyant turbulent plumes, ASME J. Heat Transfer 116 (1994) 409–417.

[9] Z. Dai, L.K. Tseng, G.M. Faeth, Velocity statistics of round, fully developed, buoyant turbulent plumes, ASME J. Heat Transfer 117 (1995a) 138–145.

[10] Z. Dai, L.K. Tseng, G.M. Faeth, Velocity/mixture fraction statistics of round, self-preserving, buoyant turbulent plumes, ASME J. Heat Transfer 117 (1995b) 918–926.

[11] Z. Dai, G.M. Faeth, Measurements of the structure of self-preserving round buoyant turbulent plumes, ASME J. Heat Transfer 118 (1996) 493–495.

[12] N.E. Kotsovinos, A study of the entrainment and turbulence in a plane buoyant jet, Ph.D. Thesis, California Institute of Technology, Pasadena, 1975.

[13] B.R. Ramaprian, M.S. Chandrasekhara, Measurements in vertical plane turbulent plumes, ASME J. Fluids Engrg. 111 (1989) 69–77.

[14] N.P. Fofnoff, Physical properties of seawater: a new salinity scale and equation of state for seawater, J. Geophys. Res. 90 (C2) (1985) 3332–3342.

[15] C.J. Chen, C.H. Chen, On the prediction and unified correlation for the decay of vertical buoyant jets, ASME J. Heat Transfer 101 (3) (1979) 532–537.

[16] A. Shabbir, D.B. Taulbee, Evaluation of turbulence models for predicting buoyant flows, ASME J. Heat Transfer 112 (1990) 945–951.

[17] M.R. Malin, B.A. Younis, Calculation of turbulent buoyant plumes with a Reynolds stress and heat flux transport closure, Int. J. Heat Mass Transfer 33 (1990) 2247–2264.

[18] D.J. Bergstrom, A.B. Strong, G.D. Stubley, Algebraic stress model prediction of a plane vertical plume, Numer. Heat Transfer A 18 (1990) 263–281.

[19] A. Dewan, J.H. Arakeri, J. Srinivasan, A new turbulence model for the axisymmetric plume, Appl. Math. Model. 21 (1997) 709–719.

[20] K. Kalita, A. Dewan, A.K. Dass, Computation of the turbulent plane plume using the $k$–$\varepsilon$–$\overline{t'^2}$–$\gamma$ model, Appl. Math. Model. 24 (2000) 815–826.

[21] S.V. Patankar, Numerical Heat Transfer and Fluid Flow, McGraw-Hill, New York, 1980.

[22] S.B. Jia, Laminar Jet Issuing into Stagnant Surroundings, CFDU, Imperial College of Science and Technology, London, 1984.

[23] C.J. Chen, W. Rodi, Vertical Turbulent Buoyant Jets, Pergamon Press, New York, 1980.

[24] A.M.Z. Alam, D.R.F. Harleman, J.M. Colonell, Evaluation of selected initial dilution models, ASCE J. Environ. Engrg. 108 (1982) 159–186.